TiS Trends in Sciences
TRENDS IN SCIENCES 2027; 24(1): 14115
SPRINT Scholarly Publishing and Repository Integration Center
https://doi.org/10.48048/tis.2027.14115
RESEARCH ARTICLE

In Vitro Verification of Increased Proton RBE In Human Malignant Meningioma Cells

Dea Aulia Kartini[1], Pharewa Karoon[1], Sasikamon Khophai[2], Taweap Sanghangthum[3], Krajang Talabnin[4], Chutima Talabnin[2] and Chinorat Kobdaj[1,*]

[1]*School of Physics, Institute of Science, Suranaree University of Technology, Nakhon Ratchasima 30000, Thailand*
[2]*School of Chemistry, Institute of Science, Suranaree University of Technology, Nakhon Ratchasima 30000, Thailand*
[3]*Division of Radiation Oncology, Department of Radiology, Faculty of Medicine, Chulalongkorn University, Bangkok 10330, Thailand*
[4]*School of Pathology, Institute of Medicine, Suranaree University of Technology, Nakhon Ratchasima 30000, Thailand*

([*]Corresponding author's e-mail: kobdaj@g.sut.ac.th)

Received: 16 April 2026, Revised: 9 June 2026, Accepted: 19 June 2026, Published: 1 August 2026

Abstract

Proton therapy is increasingly used to treat meningiomas, particularly in unresectable cases. However, studies addressing the cellular and molecular mechanisms of meningioma response to proton therapy are still limited, and the use of a generic relative biological effectiveness (RBE) value of 1.1 for meningiomas may underestimate the absorbed dose in adjacent tissues. This study aimed to address the issue of constant RBE application in clinical practice by investigating the biological effects of a pencil beam scanning, monoenergetic 100 MeV proton beam in a malignant meningioma (HKBMM) cell line and deriving the RBE specifically for meningioma through *in vitro* experiments. Cell viability, DNA damage, and survival fractions were assessed as biological endpoints following proton and X-ray irradiation, and RBE values for HKBMM cells were obtained from the clonogenic cell survival assay. A significant dose-dependent increase in γH2AX foci was observed in HKBMM cells following proton irradiation. Both X-ray and proton irradiation reduced the cell viability. However, HKBMM cells were less sensitive to X-rays than to proton beams. These findings were consistent with the measured survival curves, in which the X-ray survival curve displayed a shoulder, whereas the proton survival curve exhibited a more linear slope. Based on our clonogenic survival results, we found an $RBE_{10\%}$ of 1.28, which was higher than the constant RBE. A higher proton RBE in malignant meningiomas indicates that protons induce irreparable DNA damage. The use of accurate, tissue-specific RBE values in treatment planning can avoid excessive dose deposition in normal tissue.

Keywords: Proton therapy, Malignant meningioma, *In vitro* measurement, Clonogenic survival proton RBE, Cell viability, Double-Strand breaks

Introduction

Proton radiation therapy, which employs high-energy proton beams, has become a popular cancer treatment option. Owing to its precise dose delivery to the tumor, proton therapy offers an alternative option for malignant meningioma treatment in cases where complete removal with surgical resection is not achievable. Several clinical studies on benign meningiomas (WHO grade I) treated with proton therapy have reported survival rates of up to 90% - 100% during follow-up 5 years after treatment [1-3]. However, patients with non-benign (WHO grade II/III) meningiomas have lower survival rates and local control than those with benign meningiomas [1,4-7]. Unlike glioblastoma, which has been extensively studied as

highly aggressive and radioresistant neuro-epithelial tumors, radiobiological investigations of dose-responses and underlying molecular mechanisms of meningiomas in proton therapy remain limited. Since different cancer cell types exhibit distinct radiation responses, dedicated radiobiological studies on malignant meningioma cells treated with proton radiation are essential to characterize their specific cellular responses, rather than extrapolating from glioblastoma and other brain tumor models as proxies for all central nervous system (CNS) malignancies.

A critical point in proton therapy is that, at the same absorbed dose, the biological effect of protons differs from that of X-rays or photons. This difference was determined using the relative biological effectiveness (RBE). The RBE is defined as the ratio of the dose of a reference radiation (such as X-rays) to the dose of other radiation sources (such as protons, and carbon ions) needed to produce the same biological effect [8]. The RBE value of proton beams increases with the linear energy transfer (LET), especially towards the Bragg peak [9]. However, a constant proton RBE of 1.1 is implemented in all cancer treatment plans, despite several studies reporting variations in RBE values for various cancer types and proton LET [10]. The use of a generic proton RBE could lead to an excessive dose being delivered to the surrounding healthy tissues and organs at risk, thereby increasing the risk of complications in healthy tissues. This indicates the need for more accurate RBE data to improve treatment planning.

A previously published proton RBE study reported that the RBE values for central nervous system (CNS) meningioma based on clinical data were in the range of 1.15 - 1.16 for the minimum target RBE and 1.51 - 1.53 for the maximum target RBE; however, the RBE values based on clonogenic cell survival are not yet available [10]. Thus, relying solely on a constant RBE value for various cancer treatments will underestimate the actual dose delivered to the tumor and surrounding healthy tissue, potentially resulting in excessive dose deposition in these areas, particularly in the brain tissue. Clinical studies on proton therapy for both benign and malignant meningiomas have reported adverse outcomes, including local failure, tumor progression, brain necrosis, optical necrosis, and metastases [1,2,4,6,7].

This study aimed to address this gap by investigating the biological effects of 100 MeV monoenergetic proton beams on a human malignant meningioma cell line (HKBMM) through *in vitro* experiments. Cell survival and DNA damage following proton irradiation were evaluated using MTT, γH2AX, and colony formation assays. The results were compared with those obtained using conventional X-ray irradiation to determine the biological endpoints and obtain the proton RBE of HKBMM cells based on clonogenic cell survival. To our knowledge, this study provides the first *in vitro* evaluation of proton RBE and key radiobiological parameters (α, β, and α/β ratio) in monolayer malignant meningioma cells, thereby addressing a critical gap in proton radiobiology. Although these findings extend beyond prior CNS tumor studies primarily focused on glioblastoma models, the use of a monolayer system limits their direct applicability to complex clinical settings.

Materials and methods

Cell culture and sample preparation

The human malignant meningioma (HKBMM) cell line was kindly provided by Associate Professor Norie ARAKI (Kumamoto University, Kumamoto, Japan). HKBMM cells were cultured in complete medium consisting of Dulbecco's modified Eagle medium (DMEM), 10% fetal bovine serum (FBS), and penicillin/streptomycin in a T-25 cell culture flask (Falcon). All solutions used for cell culture were purchased from Gibco (Thermo Fisher Scientific, Waltham, MA, USA). The cells were then incubated at 37 °C in a 5% CO_2 atmosphere. The doubling time of HKBMM cells is approximately 19 h (unpublished data). 24 h before irradiation, approximately 90,000 cells were seeded as a monolayer culture in 6-well plates (SPL Life Science) containing 3 mL of medium and incubated until irradiation. Before irradiation, the wells containing the cells were filled with the medium.

Irradiation setup

For X-ray irradiation, the well plates were placed inside a box containing tissue-equivalent materials, with the well plates positioned at a source-axis distance (SAD) of 100 cm (**Figure 1(a)**). A medical linear accelerator (Varian Medical Systems, Palo, Alto, CA) was used to produce X-ray beams with an energy of 6

MV. X-ray irradiation was performed at a dose rate of 600 MU/min at doses of÷ 0, 1, 3, and 5 Gy. X-ray irradiation was performed using the anterior-posterior/posterior-anterior (AP/PA) parallel opposing technique to create a uniform dose distribution with an irradiation field size of 15×15 cm.

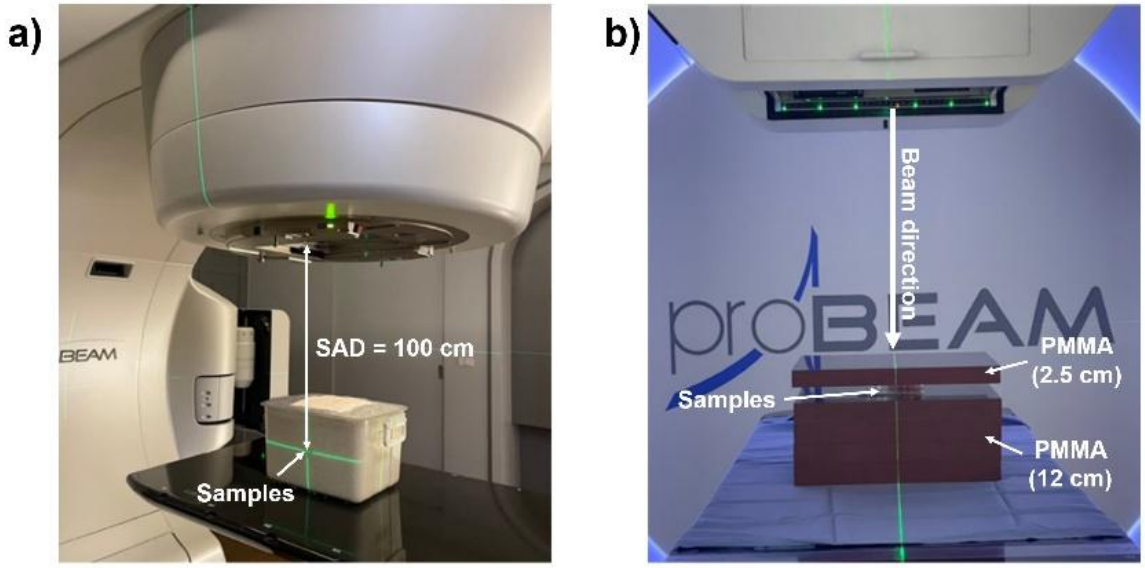


Figure 1 Experimental setup: (a) X-ray irradiation with an energy of 6 MV. The well plate containing cells were placed inside a box at a depth of 8 cm and SAD of 100 cm. (b) Proton irradiation with energy of 100 MeV monoenergetic proton beams. The well plate containing cells was placed at 3 cm depth as the normalization depth, sandwiched between PMMA slabs with thicknesses of 2.5 and 12 cm.

For the proton beam experiments, monoenergetic 100 MeV proton beams were used to irradiate the samples using pencil beam scanning at doses of 0, 1, 3, and 5 Gy. The proton beams were produced using a ProBeam Compact (Varian Medical System), which can deliver an energy range of 70 - 220 MeV for clinical irradiation. The water-equivalent thickness (WET) of the irradiation setup, consisting of a 2.5 cm PMMA slab, a 1 mm polystyrene lid, and the culture medium layer, was approximately 3 cm. At this depth, a 100 MeV proton beam remains in the plateau region of the depth-dose curve, well upstream of the Bragg peak. Therefore, the cells were irradiated under conditions where dose and LET variations across the sample were expected to be minimal. This configuration was selected to ensure a highly uniform and monoenergetic proton beam while minimizing position errors and beam-mixing complexities. An additional 12 cm of PMMA slabs were placed downstream of the sample to absorb the remaining proton energy (**Figure 1(b)**). Irradiation was performed in the AP orientation with the same field size as the X-ray plan. The two samples were irradiated simultaneously and received the same radiation dose for both X-ray and proton irradiation.

The Eclipse treatment planning system version 16.1 (Varian Medical System) was used to compute the dose calculations and create irradiation plans. For all dose calculations, a virtual water phantom of size 15×15 cm was used to achieve a homogeneous dose distribution. The AcurosXB algorithm in the Eclipse treatment planning system was used to compute the X-ray dose calculations with a calculation grid size of 0.25 cm. A proton convolution superposition algorithm was used to calculate the proton doses. Because the treatment planning system (Eclipse version 16.1) did not natively compute LET distributions, the local proton LET at the cell monolayer was estimated analytically based on the residual proton energy that hitting the target. Considering the energy degradation through the upstream materials, including the air gap between the beam nozzle and the PMMA, 25 mm PMMA slab, 1 mm polystyrene lid, and overlying culture medium, the local LET in water was calculated as follows:

$$LET = \frac{\Delta E}{\Delta x} \quad (1)$$

where ΔE is the proton energy loss across a reference water-equivalent thickness Δx. For the 100 MeV incident proton beam setup, the estimated local LET at the cell position was approximately 1.19 keV/µm.

Clonogenic assay

A clonogenic assay was performed to determine cell survival after X-ray and proton irradiation. After irradiation, the cells were immediately trypsinized using 0.25% trypsin-EDTA (Gibco). Approximately 150 - 3,000 cells (corresponding to each dose) were reseeded in triplicate in 6-well plates containing 3 mL of medium and incubated for 2 weeks. The colonies were then fixed in absolute methanol at –20 °C for 20 min and stained with 0. 5% crystal violet for 30 min. A colony of 50 cells was counted as an individual colony.

The survival fraction (SF) of cells after irradiation was determined using following Eq. (2) [11]:

$$SF = \frac{\text{Number of colonies}}{\text{Number of cell seeded} \times \text{measured PE}} \quad (2)$$

Plating efficiency (PE) was determined as the ratio of colonies formed to the number of cells seeded from the untreated sample (0 Gy). The measured survival fractions were then plotted as a function of dose and fitted using a linear-quadratic (LQ) model [12]:

$$S(D) = \exp(-\alpha D - \beta D^2) \quad (3)$$

where D is the radiation dose, and α and β are the linear and quadratic parameters of the LQ model, respectively.

MTT assay

Cell viability following X-ray and proton irradiation was determined using the MTT assay. Approximately 8,000 irradiated cells were seeded in a flat-bottom 96-well plate (SPL Life Science) and incubated for 96 h. Triplicate samples were prepared for each dose. After incubation, 10 µl of WST-8 dye (Cell Counting Kit 8 #AB228554, Abcam) was added to each well and the plate was incubated for 1 h. Optical density (*OD*) was measured using a TECAN Infinite 200 Pro microplate reader at a wavelength of 460 nm. The percentage of viable cells was calculated as follows:

$$\text{Cell viability} = \frac{OD_{\text{treated sample}}}{OD_{\text{control sample}}} \times 100 \quad (4)$$

Immunofluorescent staining of phosphor-histone H2AX (γH2AX assay)

To evaluate persistent, unrepaired DNA double-strand breaks (DSBs), which serve as indicators of lethal cellular damage and correlate with long-term cell survival end points, the γH2AX assay was performed 72 h post-irradiation according to the following protocol. Irradiated cells were seeded at a density of 24,000 cells on an 8-well chamber slide (SPL Life Science) and incubated for 72 h. The cells were fixed in 4% formaldehyde in PBS for 15 min, permeabilized with 0.1% Triton X-100 in PBS (PBST) on ice for 10 min, and washed with PBS. Subsequently, the cells were blocked with 2% BSA in 0.1% PBST (0.1% Tween20) on ice for 30 min and incubated with the primary antibody (γH2AX #80312, Cell Signaling Technology, USA) overnight at 4 °C. The cells were washed with 0.1% PBST, incubated with a secondary antibody (Anti-mouse IgG-AlexaTM 647 #4410S, Cell Signaling Technology, USA) for 30 min, and washed with 0.1% PBST. Subsequently, the cell nuclei were stained using a nuclear counterstain with Hoechst 33258 solution (1:1,000) for 10 min and washed with 0.1% PBST. The γH2AX foci were examined using a confocal laser scanning microscope (Nikon, Tokyo, Japan).

Statistical analysis

A two-way analysis of variance was used to calculate the significance between the X-ray and proton samples using GraphPad Prism Software (version 10.3.1; GraphPad Software, Inc.). $p < 0.05$ was considered statistically significant, while the p-values $p \geq 0.05$ was considered not significant (ns).

Results and discussion

Effect of proton radiation on DNA damage in HKBMM cells

In this study, the γH2AX assay was performed to observe DNA damage in HKBMM cells 72 h after irradiation. **Figure 2(a)** shows representative images of Hoechst staining corresponding to the nuclei of HKBMM cells and γH2AX staining corresponding to

DNA damage foci (pink spots). γH2AX foci refer to the phosphorylation of histone H2AX close to DNA double-strand breaks (DSBs); thus, the number of DNA DSBs is usually equal to the number of γH2AX foci [13-15].

The number of γH2AX foci increased with increasing radiation dose. The number of γH2AX foci per nucleus at different radiation doses is presented in **Figure 2(b)**. The baseline-subtracted γH2AX foci per 100 nuclei for cells exposed to 1 and 3 Gy of X-rays were 0.28 ± 0.10 and 0.62 ± 0.25, respectively. Following 5 Gy of X-ray irradiation, the number of foci increased to 3.43 ± 2.69 per 100 nuclei. In contrast to X-ray beams, induced significantly higher yields of DNA damage, especially at doses of 3 and 5 Gy. The number of γH2AX foci per 100 nuclei following 1, 3, and 5 Gy of proton beam irradiation was 8.92 ± 2.75, 19.70 ± 8.52, and 43.8 ± 13.0, respectively.

The number of γH2AX foci increased significantly with increasing proton dose, indicating that proton beams induce more DSBs than X-ray beams do [16-18]. Previous studies have reported that γH2AX foci induced by high-LET radiation remained for more than 24 h longer than those induced by low LET radiation (γ-ray and X-ray). This is because the damage caused by high-LET radiation is much more complicated and difficult to repair [19,20]. Our results showed that proton-induced γH2AX foci were still visible 72 h after irradiation. This suggests that DNA damage caused by proton radiation is more difficult to repair than that caused by X-ray radiation.

Cell-killing effect of proton radiation in HKBMM cells

The MTT assay was performed 96 h after X-ray and proton irradiation to measure cellular metabolic activity, which serves as an indicator of viable cells following irradiation [21]. All the measured data were normalized to the control sample. **Figure 3** shows the viability of HKBMM cells following X-ray and proton irradiation. Cells showed a gradual decrease in viability as the X-ray dose increased, and cell viability dropped to 61% after irradiation with 5 Gy X-ray beams. Meanwhile, the cells showed a significant decrease in cell viability after proton irradiation, with the lowest cell viability of 48% after irradiation with 5 Gy proton beams.

The cell survival fractions following X-ray and proton irradiation were determined using a clonogenic assay and computed using Eq. (2). The plating efficiency values of the HKBMM cells were 0.7300 and 0.5611 for X-ray and proton irradiation, respectively. Next, the survival curves of the HKBMM cells were plotted, and the survival fractions were fitted using the linear-quadratic model in Eq. (3) (**Figure 4**). The measured X-ray survival curve (red curve) showed a shoulder in the low-dose region, with the survival fractions gradually decreasing in the high-dose region. The shoulder–of the X-ray survival curve implies that sub-lethal DNA damage (such as single-strand breaks) from low-dose radiation (≤ 1 Gy) could be repaired. However, cell repair systems cannot fix the complex lethal DNA damage caused by high-dose radiation, resulting in a significant decline in cell survival. This result is in good agreement with the cell viability measured using the MTT assay, where cells exposed to low-dose radiation showed a higher survival rate than those exposed to high-dose radiation, confirming the relationship between dose and cell death.

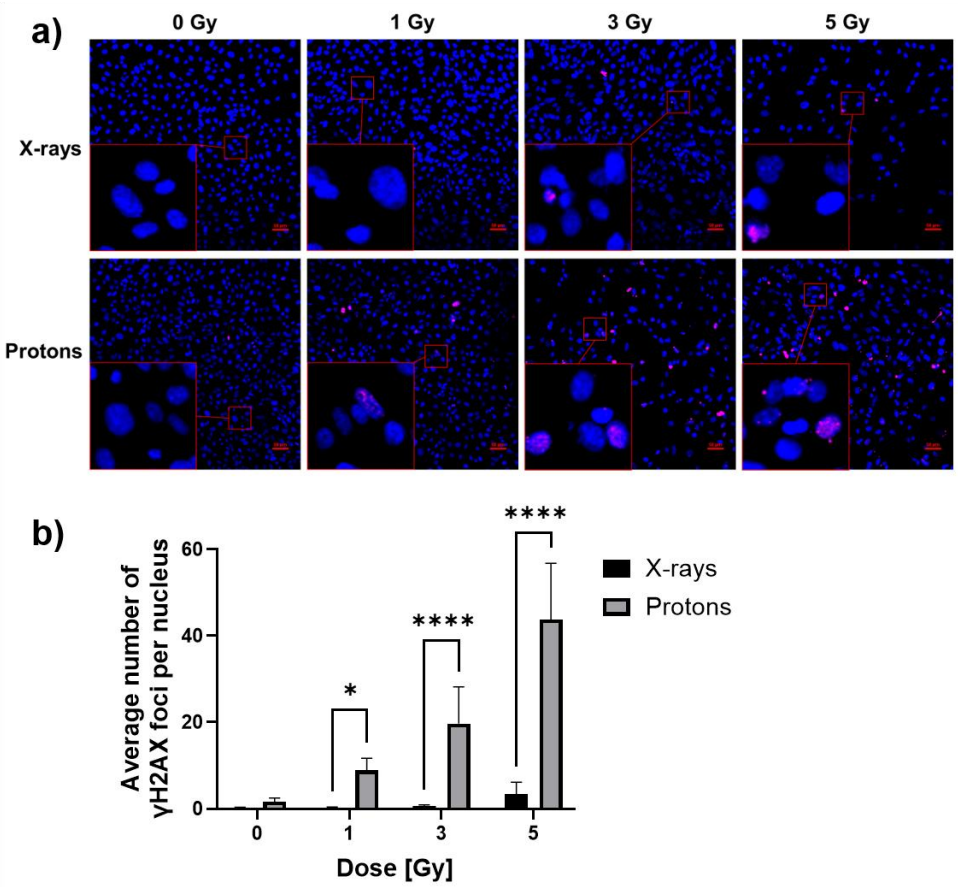


Figure 2 DNA damage of HKBMM cells at 72 h after the X-ray and proton irradiations. (a) Representative images of HKBMM cells after X-ray and proton irradiations. Hoechst staining represents nuclei of HKBMM cells (blue color) and γH2AX staining represents DNA damage (pink spots). Magnification: 20X, scale bar represents 50 µm. (b) The average number of γH2AX foci per nucleus corresponding to each irradiation dose was shown as mean ± SD (n = 4). Significant difference $*p = 0.0416$ X-rays vs proton at 1 Gy, $****p < 0.0001$ X-rays vs proton at 3 and 5 Gy.

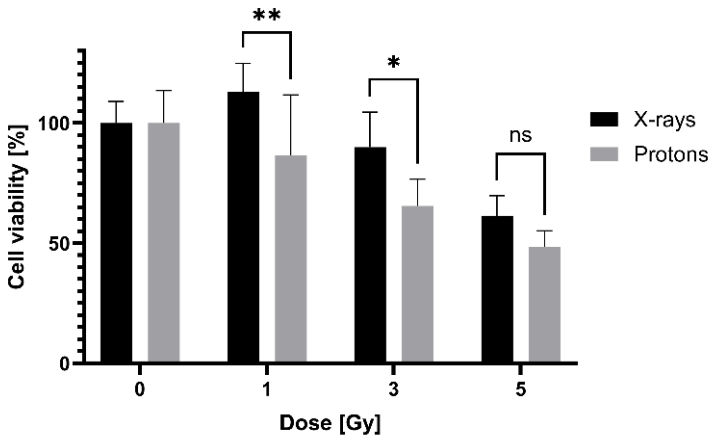


Figure 1 Measured cell viability of HKBMM cells at 96 h after X-ray and proton irradiations. All data have been normalized to the control sample and presented in percentages. The values were represented as mean ± SD (n = 6). Significant difference $**p < 0.007$ X-rays vs proton at 1 Gy, $*p < 0.0135$ X-rays vs proton at 3 Gy.

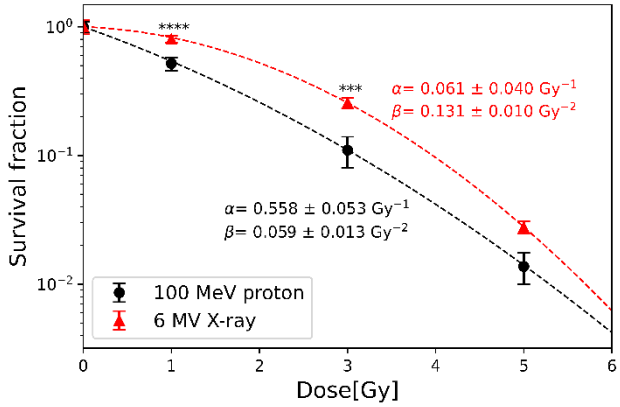


Figure 4 Survival curves of HKBMM cells after irradiation using pencil beam scanning, monoenergetic 100 MeV proton (LET ≈1.19 keV/μm) and 6 MV X-ray beams. Symbols ● and ▲ corresponding to the survival fractions of cells following proton and X-ray irradiations, respectively. The dashed lines corresponding to the fit of data using LQ model: $SD = exp(-\alpha D - \beta D^2)$. The values were represented as mean ± SD (n = 6). Significant difference $****p < 0.0001$ X-rays vs proton at 1 Gy, $***p = 0.0003$ X-rays vs proton at 3 Gy.

The measured proton curve (black curve) exhibited a steeper slope with decreasing survival fraction. This steep decline in survival fractions aligns with the persistent, complex DNA damage observed at 72 h. These findings are consistent with the α and β parameters presented in **Table 1**. The α parameter represents lethal and irreparable damage from a single radiation track, whereas the β parameter represents the damage caused by the interactions of multiple radiation tracks [22]. Based on **Table 1**, the α parameter of the proton curve is higher than the β parameter, resulting in a higher α/β ratio of 9.41 compared to the X-ray survival curve (0.46). The higher α/β ratio of proton beams indicates that cell death is dominated by irreparable single-track events, making HKBMM cells more sensitive to proton radiation. However, it should be noted that these α and β values were derived from a limited number of dose points within a single cell line. Thus, these specific α/β values are highly cell line-dependent, highlighting the limitations of using them to define the precise underlying biophysical mechanism of cell death.

Table 1 Measured α and β values with 95% CI, α/β ratio, and standard deviation of regression (S_e) of X-ray and proton survival curves.

Irradiation	α (Gy^{-1}) [95% CI]	β (Gy^{-2}) [95% CI]	α/β (Gy)	S_e
6 MV X-rays	0.061 ± 0.040 [–0.232, 0.111]	0.131 ± 0.010 [–0.174, –0.088]	0.46	0.025
100 MeV monoenergetic protons	0.558 ± 0.053 [–0.788, –0.329]	0.059 ± 0.013 [–0.117, –0.002]	9.41	0.033

Abbreviations: CI, confidence interval; S_e, standard error of the estimate (standard deviation of regression). The 95% CIs were reconstructed using the exact critical value $t_{0.05,4} = 4.303$ based on 4 dose groups with 6 replicates each.

Measured $RBE_{10\%}$ of HKBMM cells and RBE as function of dose

In proton therapy, the biological effects differ from those of X-rays at the same absorbed dose. Thus, the application of RBE in proton therapy is necessary to translate proton doses into biologically equivalent doses for X-ray therapy. The RBE value of the HKBMM cells was obtained from the measured survival curves using Eq. (5). The doses from X-ray and proton irradiation that resulted in 10% cell survival were compared, and we found that the RBE at 10% cell survival ($RBE_{10\%}$) was 1.28 for HKBMM cell survival.

$$\text{RBE} = \frac{\text{Dose}_{\text{X-rays}}}{\text{Dose}_{\text{Protons}}} \quad (5)$$

The proton RBE is dependent on several factors, including LET, beam energy, radiation dose, and the specific tissue type [23,24]. In this study, the estimated local LET at the irradiation position was approximately 1.19 keV/µm. According to our clonogenic survival results, the measured $\text{RBE}_{10\%}$ for HKBMM cells in this entrance channel was 1.28, which is notably higher than the clinical RBE value (1.1) [9,23]. These findings are consistent with the general RBE trends reported for other tumor models (**Figure 5**). However, it is important to emphasize that the compiled RBE values in **Figure 5** originate from fundamentally different biological and methodological contexts, including clinical observations and *in vitro* clonogenic assays. Direct comparison should therefore be interpreted with caution, as *in vitro* cell survival parameters do not capture all the complexity of tissue-tissue responses in a clinical setting. Consequently, these comparisons are useful for identifying RBE trends but cannot be used directly to define definite clinical RBE for meningiomas.

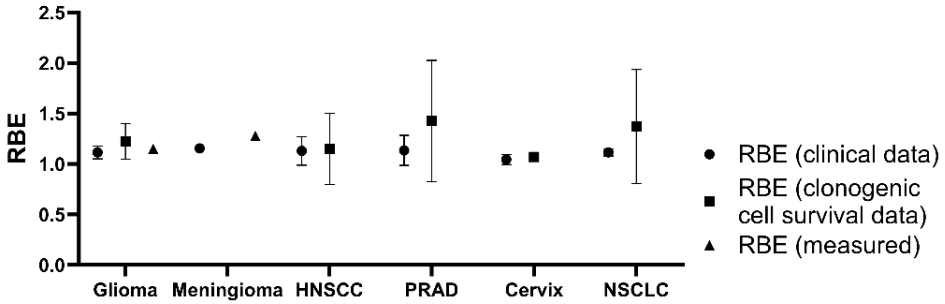


Figure 2 RBE values of different cancer types based on clinical data ●, clonogenic cell survival data *in vitro* ■, and measured cell survival data ▲. Clinical data- and clonogenic *in vitro* data-based RBE values were obtained from published RBE study by Paganetti, H. (2021) [10]. Measured cell survival data-based RBE for glioma was obtained from previously published study [25]. *Abbreviations*: HNSCC = head and neck squamous cell carcinoma, PRAD = prostate adenocarcinoma, NSCLC = non-small cell lung cancer.

RBE in the brain, especially within the tumor site, is expected to be higher owing to the increase in LET as protons approach the tumor, thereby increasing the risk of brain injury [26]. This potential for a higher RBE at the tumor site means that the use of a constant RBE value (1.1) can lead to an underestimation of the biologically effective dose delivered to the tissue, increasing toxicity in healthy brain tissue. Clinical evidence highlights these risks across various cohorts. Murray *et al*. [1] reported a study of 96 patients with WHO grade I-III meningiomas, where two patients experienced brain necrosis [1]. Similarly, Song *et al*. [26] observed that out of 38 patients who received proton therapy, three developed brain necrosis and one developed white matter lesions [26]. Furthermore, a long-term clinical study by Krcek *et al*. [6] evaluating the clinical outcomes of proton therapy in WHO grade I-III meningiomas between 1997 and 2022 highlighted late severe toxicities (≥ grade 3), including visual toxicity, cataracts, brain necrosis, ear and labyrinth disorders, stroke, brain edema, pain exacerbation, and pituitary dysfunction [6].

Figure 5 presents a compilation of RBE values derived from clinical and *in vitro* clonogenic cell survival data across various cancer cells, including CNS gliomas and meningiomas, demonstrating that most RBE values exceed the standard clinical RBE [10]. For CNS meningiomas, specific RBE values based on clonogenic cell survival data were previously unavailable, and our findings can be included in the RBE database for future RBE-based treatment planning studies. Besides defining tumor radiosensitivity, optimizing proton therapy requires careful consideration of the RBE for normal brain tissue. Zhou *et al*. [27] assessed the proton RBE variations in the hippocampus of Sprague-Dawley rats following high dose proton irradiation, reporting an RBE of 1.65 for neurons, a range between 1.1 and 1.65 for oligodendrocytes and

microglia, and a standard 1.1 for neural stem cells [27]. On the other hand, an evaluation of different intracerebral cell types in a rabbit model by Wang *et al*. [28] indicated that the RBE values for neurofilaments and oligodendrocytes fell below 1.1 under their experimental conditions [28]. These divergent values imply that normal tissue toxicity is governed by complex and cell-specific radiosensitivities that require careful integration into variable RBE planning algorithms.

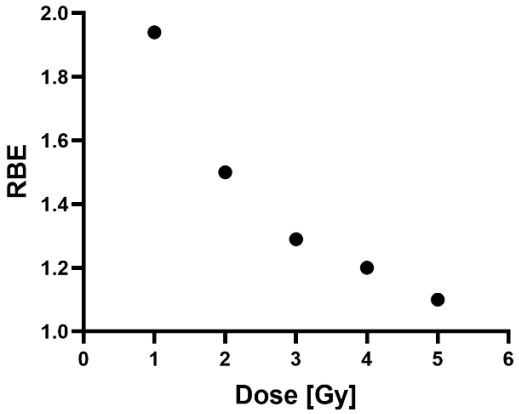


Figure 6 Measured proton RBE of HKBMM cells as a function of dose following irradiation using a pencil beam scanning, monoenergetic 100 MeV proton beam (LET ≈1.19 keV/μm) in the entrance channel.

To further understand the RBE, the dose-dependence of the proton RBE was investigated. **Figure 6** shows the measured proton RBE as a function of the radiation absorbed dose after irradiation using monoenergetic 100 MeV proton beams at the entrance channel. By using Eq. (3), we obtained RBE_{2Gy} value of 1.5, whereas for doses below 2 Gy, the RBE values further increased, reaching up to 1.94. This increase in the RBE values with decreasing proton dose for HKBMM cell survival is consistent with a previously published proton RBE study [9].

Given that RBE depends strongly on proton energy, LET, and specific cell types, a comprehensive understanding requires assessment under multiple irradiation conditions. In this study, proton irradiation was intentionally restricted to the entrance plateau region using a monoenergetic beam. While this setup is ideal for establishing a baseline cellular response relative to X-rays without the added variables of mixed-energy fields, it underrepresents the elevated LET and heightened RBE values observed at the Bragg peak and its distal edge. Since clinical proton therapy exploits the high biological effectiveness along the SOBP, future investigations evaluating cell survival across diverse cell lines at multiple positions along the SOBP are necessary to fully assess maximum clinical efficacy.

Furthermore, it should be noted that this study evaluated a single malignant meningioma model grown as a flat monolayer. While these data offer an essential foundation for proton-induced cell death in meningiomas, future research should include broader patient-derived lines and other high-grade meningioma models to fully validate the generalizability of these radiobiological parameters. Additionally, because our findings are based on monolayer *in vitro* cultures, further studies using 3D culture models are necessary to provide more biologically relevant cell survival data, as cells grown in 3D environments are far more representative of biological tissues. Given that cells in 3D culture are known to exhibit increased radio resistance compared to cells grown as flat monolayers, their RBE values may indeed be significantly different, making this a critical research focus for future translation into clinical treatment planning [25,29].

From a translational perspective, obtaining precise and accurate radiosensitivity parameters (α, β, and α/β ratio) for malignant meningiomas is directly relevant for clinical treatment planning. Currently, a fixed RBE value of 1.1 is applied in standard proton therapy. However, meningiomas are frequently located in close proximity to organs at risk (OAR), such as the optic nerves and brainstem. Thus, applying dedicated cell

survival parameters for malignant meningioma cells can help to refine radiobiological modeling for proton therapy. Accurately mapping these tissue-specific responses is an important step toward moving forward from fixed RBE to variable RBE models, thereby improving tumor control while minimizing late toxicities in surrounding healthy brain tissues. While the γH2AX assay is a gold-standard method for quantifying double-strand breaks, the evaluation in this study was limited to a single, late time point (72 h) without co-staining factors such as 53BP1. Although this endpoint is ideal for measuring lethal residual DNA damage, future studies evaluating DNA DSBs repair kinetics at multiple time points will be valuable for fully characterizing the DNA repair rates of meningioma cells following proton irradiation.

Conclusions

This study aimed to provide further insights into *in vitro* research on human malignant meningioma cell lines after irradiation with monoenergetic 100 MeV protons and 6 MV X-ray beams. A significant decrease in both cell viability and survival fractions was observed following proton irradiation, indicating that irreparable damage leads to cell death. Based on our clonogenic cell survival results, the proton $RBE_{10\%}$ in the entrance channel was determined to be 1.28. While these *in vitro* monolayer findings suggest that the biological effectiveness of protons may exceed the generic proton RBE (1.1), they reflect a simplified cellular model that does not account for the complexities of the 3D tumor microenvironment. Therefore, these results cannot be directly translated into clinical settings. Further investigations using diverse cell lines, 3D culture environments, and advanced radiobiological models are required before variable RBE can be incorporated into clinical proton treatment planning.

Acknowledgements

This work was supported by Suranaree University of Technology (SUT) Nakhon Ratchasima 30000, Thailand; Thailand Science Research and Innovation (TSRI); National Science, Research and Innovation Fund (NSRF) (NRIIS number 204211); NSRF via the Program Management Unit for Human Resources & Institutional Development, Research and Innovation Fund (grant number B39G680009); and Center of Excellence in High Energy Physics and Astrophysics. Dea Aulia Kartini is additionally supported by SUT under the Full-Time Doctoral Researcher grant (Full-time66/21/2566). The authors would like to thank Dr. Tanawat Tawonwong and Jaruek Kanphet for operating the X-ray linear accelerator at KCMH.

Declaration of generative AI in scientific writing

The authors acknowledge the use of generative AI tools (e.g., QuillBot and Google Gemini by OpenAI) in the preparation of this manuscript, specifically for language editing and grammar correction. No content generation or data interpretation was performed by AI. The authors take full responsibility for the content and conclusions of this work.

CRediT author statement

Dea Aulia Kartini: Conceptualization; Methodology; Formal Analysis; Investigation; Writing - Original draft preparation. **Pharewa Karoon**: Methodology; Formal Analysis; Investigation; Writing - Original draft preparation. **Sasikamon Khophai**: Investigation. **Taweap Sanghangthum**: Investigation; Resources; Writing - Reviewing and Editing. **Krajang Talabnin**: Resources; Supervision. **Chutima Talabnin**: Formal Analysis; Resources; Supervision; Writing - Reviewing and Editing. **Chinorat Kobdaj**: Resources; Supervision; Writing - Reviewing and Editing; Funding acquisition.

References

[1] FR Murray, JW Snider, A Bolsi, AJ Lomax, M Walser, U Kliebsch, RA Schneider and DC Weber. Long-term clinical outcomes of pencil beam scanning proton therapy for benign and non-benign intracranial meningiomas. *International Journal of Radiation Oncology, Biology, Physics* 2017; **99(5)**, 1190-1198.

[2] RAE Shafie, M Czech, KA Kessel, D Habermehl, D Weber, S Rieken, N Bougatf, O Jäkel, J Debus and SE Combs. Clinical outcome after particle therapy for meningiomas of the skull base: Toxicity and local control in patients treated with active rasterscanning. *Radiation Oncology* 2018; **13**, 54.

[3] H Sato, M Mizumoto, T Okumura, H Sakurai, N Sakamoto, H Akutsu, E Ishikawa and K Tsuboi.

Long-term outcomes of patients with unresectable benign meningioma treated with proton beam therapy. *Journal of Radiation Research* 2021; **62(3)**, 427-437.

[4] MW McDonald, DA Plankenhorn, KP McMullen, MA Henderson, EJ Dropcho, MV Shah and AA Cohen-Gadol. Proton therapy for atypical meningiomas. *Journal of Neuro-Oncology* 2015; **123**, 123-128.

[5] C Champeaux-Depond and J Weller. Outcome after protontherapy for progression or recurrence of surgically treated meningioma. *Brain Tumor Research and Treatment* 2021; **9(2)**, 46-57.

[6] R Krcek, D Leiser, M García-Marqueta, A Bolsi and DC Weber. Long term outcome and quality of life of intracranial meningioma patients treated with pencil beam scanning proton therapy. *Cancers* 2023; **15(12)**, 3099.

[7] A Iannalfi, G Riva, S Lillo, L Ciccone, G Fontana, S Molinelli, L Trombetta, M Ciocca, S Imparato, M Pecorilla and E Orlandi. Proton therapy for intracranial meningioma: A single-institution retrospective analysis of efficacy, survival and toxicity outcomes. *Journal of Neuro-Oncology* 2024; **169**, 683-692.

[8] J Valentin. Relative biological effectiveness (RBE), quality factor (Q), and radiation weighting factor (w_R): ICRP Publication 92: Approved by the Commission in January 2003. *Annals of the ICRP* 2003; **33(4)**, 1-117.

[9] H Paganetti. Relative biological effectiveness (RBE) values for proton beam therapy. Variations as a function of biological endpoint, dose, and linear energy transfer. *Physics in Medicine & Biology* 2014; **59(22)**, R419-R472.

[10] H Paganetti. Mechanisms and review of clinical evidence of variations in relative biological effectiveness in proton therapy. *International Journal of Radiation Oncology, Biology, Physics* 2022; **112(1)**, 222-236.

[11] NAP Franken, HM Rodermond, J Stap, J Haveman and CV Bree. Clonogenic assay of cells *in vitro*. *Nature Protocols* 2006; **1**, 2315-2319.

[12] EJ Hall and AJ Giaccia. *Radiobiology for the radiologist: Seventh edition*. Lippincottt Williams & Wilkins, Philadelphia, 2011.

[13] V Valdiglesias, S Giunta, M Fenech, M Neri and S Bonassi. γH2AX as a marker of DNA double strand breaks and genomic instability in human population studies. *Mutation Research/Reviews in Mutation Research* 2013; **753(1)**, 24-40.

[14] Y Lee, Q Wang, I Shuryak, DJ Brenner and HC Turner. Development of a high-throughput γ-H2AX assay based on imaging flow cytometry. *Radiation Oncology* 2019; **14**, 150.

[15] QT Ostrom, M Price, C Neff, G Cioffi, KA Waite, C Kruchko and JS Barnholtz-Sloan. CBTRUS statistical report: Primary brain and other central nervous system tumors diagnosed in the United States in 2015 - 2019. *Neuro-Oncology* 2022; **24(5)**, v1-v95.

[16] L Wang, X Wang, Y Li, S Han, J Zhu, X Wang, DP Molkentine, P Blanchard, Y Yang, R Zhang, N Sahoo, M Gillin, XR Zhu, X Zhang, JN Myers and SJ Frank. Human papillomavirus status and the relative biological effectiveness of proton radiotherapy in head and neck cancer cells. *Head & Neck* 2016; **39(4)**, 708-715.

[17] B Lohberger, D Glänzer, N Eck, S Kerschbaum-Gruber, E Mara, S Deycmar, T Madl, K Kashofer, P Georg, A Leithner and D Georg. Activation of efficient DNA repair mechanisms after photon and proton irradiation of human chondrosarcoma cells. *Scientific Reports* 2021; **11**, 24116.

[18] Q Akolawala, M Rovituso, HH Versteeg, AMR Rondon and A Accardo. Evaluation of proton-induced DNA damage in 3D-engineered glioblastoma microenvironments. *ACS Applied Materials & Interfaces* 2022; **14(18)**, 20778-20789.

[19] T Groesser, H Chang, G Fontenay, J Chen, SV Costes, MH Barcellos-Hoff, B Parvin and B Rydberg. Persistence of γ-H2AX and 53BP1 foci in proliferating and non-proliferating human mammary epithelial cells after exposure to γ-rays or iron ions. *International Journal of Radiation Biology* 2011; **87(7)**, 696-710.

[20] K Oonishi, X Cui, H Hirakawa, A Fujimori, T Kamijo, S Yamada, O Yokosuka and T Kamada. Different effects of carbon ion beams and X-rays on clonogenic survival and DNA repair in human pancreatic cancer stem-like cells. *Radiotherapy and Oncology* 2012; **105(2)**, 258-265.

[21] M Ghasemi, T Turnbull, S Sebastian and I Kempson. The MTT assay: Utility, limitations, pitfalls, and interpretation in bulk and single-cell analysis. *International Journal of Molecular Sciences* 2021; **22(23)**, 12827.

[22] SJ McMahon. The linear quadratic model: Usage, interpretation and challenges. *Physics in Medicine & Biology* 2019; **64(1)**, 01TR01.

[23] H Paganetti, A Niemierko, M Ancukiewicz, LE Gerweck, M Goitein, JS Loeffler and HD Suit. Relative biological effectiveness (RBE) values for proton beam therapy. *International Journal of Radiation Oncology, Biology, Physics* 2002; **53(2)**, 407-421.

[24] International Atomic Energy Agency. *Relative biological effectiveness in ion beam therapy*. International Atomic Energy Agency, Vienna, Austria, 2008.

[25] DA Kartini, P Karoon, Y Malad, T Tippayamontri, T Sanghangthum, C Talabnin and C Kobdaj. Human glioblastoma (U87) cells grown in 3D culture showed a radio-resistance to X-ray and proton radiation. *Radiological Physics and Technology* 2025; **18**, 688-697.

[26] J Song, S Aljabab, L Abduljabbar, YD Tseng, JK Rockhill, JR Fink, L Chang and LM Halasz. Radiation-induced brain injury in patients with meningioma treated with proton or photon therapy. *Journal of Neuro-Oncology* 2021; **153**, 169-180.

[27] S Zhou, X Ding, Y Zhang, Y Liu, X Wang, Y Guo, J Zhang, X Liu, G Gong, Y Su, L Wang, M Zhao and M Hu. Evaluation of specific RBE in different cells of hippocampus under high-dose proton irradiation in rats. *Scientific Reports* 2024; **14**, 8193.

[28] X Wang, Y Guo, J Zhang, M Zhao, Y Liu, X Liu, X Ding, S Zhou, X Yin, J Zhu, Y Zhang, G Gong, L Wang, Y Su, T Sun, NY Lee, J Yu and M Hu. Dose-and time-dependent relative biological effect of proton in different intracerebral cells. *Scientific Reports* 2026; **16**, 8984.

[29] DA Kartini, O Sokol, J Wiedemann, W Tinganelli, M Witt, G Camazzola, M Krämer, C Talabnin, C Kobdaj and MC Fuss. Validation of a pseudo-3D phantom for radiobiological treatment plan verifications. *Physics in Medicine & Biology* 2020; **65(22)**, 225039.